

Article

Post Synthetic Defect Engineering of UiO-66 Metal-Organic Framework with Iridium(III)-HEDTA Complex and Application in Catalysis for Water Oxidation

Giordano Gatto¹, Alceo Macchioni^{1*}, Roberto Bondi¹, Fabio Marmottini¹ and Ferdinando Costantino^{1,*}

¹ Department of Chemistry, Biology and Biotechnology, Università di Perugia and CIRCC, Via Elce di Sotto, 8, I-06123, Perugia, Italy

* Correspondence: alceo.macchioni@unipg.it;ferdinando.costantino@unipg.itTel.: +39-075-585-5579 (A. M.); +39-075-585-5563 (F. C.)

Abstract: Clean production of renewable fuels is a great challenge of our scientific community. Iridium complexes have demonstrated a superior catalytic activity in the water oxidation (WO) reaction, which is a crucial step in water splitting process. Herein we have used a defective zirconium MOF with UiO-66 structure as support of a highly active Ir complex based on EDTA with formula [Ir(HEDTA)Cl]Na. The defects are induced by the partial substitution of terephthalic acid with smaller formate groups. Anchoring of the complex occurs through a post-synthetic exchange of formate anions, coordinated at the zirconium clusters of the MOF, with the free carboxylate group of the [Ir(HEDTA)Cl]-complex. The modified material was tested as heterogeneous catalyst for the WO reaction by using Cerium Ammonium Nitrate as sacrificial agent. Although TOF and TON values are comparable to those of other iridium heterogenized catalysts, the MOF exhibits iridium leaching not limited at the first catalytic run, as usually observed, suggesting a lack of stability of the hybrid system under strong oxidative conditions.

Keywords: Metal-Organic Framework; Post-Synthetic Modification; Iridium Catalysis; Water Oxidation; Water Splitting

1. Introduction

Water oxidation (WO) to molecular oxygen is considered the ideal reaction to provide electrons and protons for the generation of renewable fuels.^[1-3] In addition to be thermodynamically disfavored, WO is also an extremely complicated, multi-electrons and multi-protons, reaction from the kinetic point of view, asking for an efficient and robust catalyst (C).^[4] WOCs based on iridium are among the most efficient reported in the literature so far, having, however, in the little abundance and, consequently, high cost of iridium their "Achille's heel".^[5-7] A possible strategy to alleviate this problem stems in the minimization of the amount of noble-metal exploited in the catalytic process, according to the noble-metal atom economy principle.^[5] This can be accomplished by utilizing i) extremely active molecular catalysts at very low concentration,^[8-15] ii) layered heterogeneous catalyst in which almost all active sites are reachable by the substrate^[16] and iii) heterogenized hybrid materials derived from the anchoring a well-defined molecular catalyst on a suitable support.^{[17][18]} The latter strategy should guarantee a very high percentage of active sites (potentially 100%), increased robustness of catalyst, mainly due to the inhibition of associative deactivation processes, and possible beneficial cooperation between the anchored catalyst and support. Many hybrid heterogenized catalysts have reported in the literature^[17,19-23] and, among them, those using MOF as support, pioneered by Lin and co-workers,^[24,25] have been particularly successful.^[26] MOFs are a class

of porous crystalline compounds constituted of the ordered connection of metal-clusters and organic linkers, forming accessible pores and channels potentially useful for a plethora of applications.^[27-29] Some of them are rapidly approaching the industrial world.^[30] Zr-MOFs are particularly interesting for their chemical and thermal stability and low production cost. The archetype structure is that of UiO-66 which is constituted of hexanuclear clusters of formula $Zr_6O_4(OH)_4(BDC)_6$ ¹²⁺ (BDC= 1,4-benzenedicarboxylic acid) in a cubic framework with **fcu** topology.^[31] This MOF possess the exotic feature to be defective when it is crystallized in the presence of a mono carboxylic modulator such as formic, acetic or benzoic acid, which act as substituent of bdc linker attached to the Zr_6 cluster thus inducing missing linker defects into the structure. These defects can be considered as an opportunity to be employed for imparting targeted functionality to the MOFs by means the so called Post-Synthetic Defect Exchange (PSDE) of the monocarboxylic groups with other carboxylic linkers.^[32,33]

Herein we report on the synthesis of formic acid (FA) modulated UiO-66 with a high concentration of defects and its use as a support for anchoring, by means of PSDE, an Ir(III) WOC complex based on EDTA (EDTA = N,N,N',N'-Ethylenediaminetetracetic acid). The complex, of formula $[Ir(HEDTA)Cl]Na$ (see fig. 1) was already reported in literature as an efficient and durable homogeneous WOC under chemical oxidation with cerium ammonium nitrate as sacrificial agent.^[34] The molecular structure of the complex clearly shows that it possess a free carboxylic group which could be employed as an anchoring functionality for its deposition onto solid surface. Our approach here consists in a PSDE of the FA-UiO-66 MOF with the $[Ir(HEDTA)Cl]$ complex dissolved in water. The anchoring occurred through a topotactic exchange of the coordinated FA with the carboxylic group of the IrCl-EDTA complex. The hybrid material (IrEDTA@UiO-66) was characterized by means of surface area and porosity studies, ICP analysis, NMR spectroscopy and tested for WO reaction by using CAN as sacrificial agent. The hybrid exhibited WO activity with TOF and TON values comparable to those of the best performing materials. However, a significant Ir leaching was observed not only during the first catalytic run, as usually observed, suggesting that strong oxidative conditions with Ce^{4+} leads to a rapid decomposition of the hybrid material.

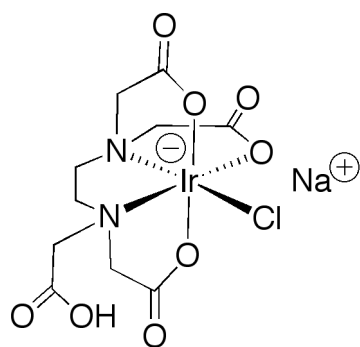


Figure 1. Molecular structure of $[Ir(HEDTA)Cl]Na$ complex

2. Results and discussion

2.1. Synthesis and characterization

2.1.1. Synthesis of FA-modulated UiO-66

FA-modulated UiO-66 was prepared according to the paper of Taddei et al.^[23] The use of large amount of formic acid as modulator (100 eq. respect to Zr) induced the formation of a highly defective phase respect to the defective free UiO-structure, which can be obtained following other synthetic strategies present in literature.^[35] FA acts as monocarboxylic modulator with the Zr clusters inducing two types of defects: missing linker defects (fig.2b) and missing cluster defects (fig.2c).

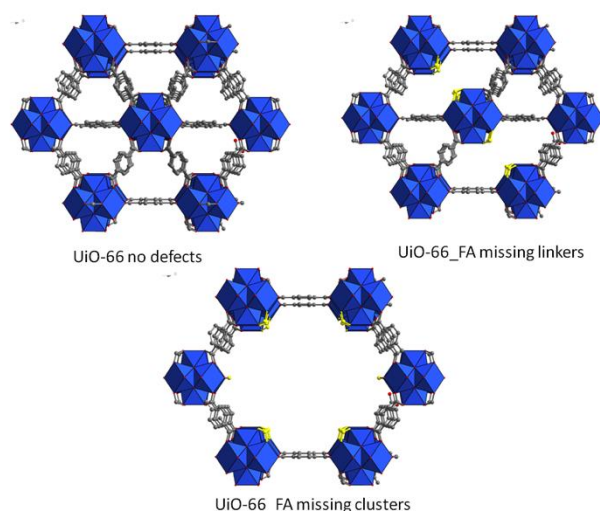


Figure 2. Structure of non-defective (a), missing linker defective (b) and missing cluster defective (c) UiO-66 phase. Formic acid is evidenced in yellow.

It is known that the materials obtained with FA as modulator possess most likely missing cluster defects.^[33] Nitrogen adsorption and desorption analysis at 77K was performed on FA-UiO-66 compound after activation at 120 °C overnight. The N₂ adsorption/desorption isotherm is reported in figure 3a and the BET value is 1450 m²/g with a total micropore volume of 0.57 cm³/g. These values, quite higher than the normal surface area and micropore volume of a defect-free UiO-66 (about 1100 m²/g and 0.4 cm³/g), confirm the highly defective nature of the obtained material. XRPD pattern of FA-UiO-66 (fig. 3b) shows the peaks at 7.3 and 8.2 ° of 2θ belonging to the (111) and (200) of the **fcu** UiO-66 phase, and a remarkable crystallinity degree. ¹H-NMR spectra on the hydrolyzed compound (fig. 3b) confirm the presence of a considerable amount of FA, as can be seen in figure 3d. Integration of ¹H-NMR signals belonging to formic acid (8.3 ppm) and terephthalic acid (7.8 ppm) gives a FA/BDC ratio equal to 0.63. The obtained solution after the hydrolysis of the sample with NaOH was analysed by ion chromatography resulting the following BDC and FA contents in the starting solid: BDC = 2.78 mmol/g and FA = 1.72 mmol/g.

Given these results, the ratio FA/BDC = 0.63 is in very good agreement with the results of NMR experiments. Since FA is a monocarboxylic acid, the following equation can be used in order to determine the formula of the defective MOF:

$$\frac{FA}{BDC} = \frac{2x}{6-x} = 0,62$$

Resulting in Zr₆O₄(OH)₄(BDC)_{4.58}(FA)_{2.74}. Thermogravimetric analysis (fig. 3c) shows three different weight losses at 100 °C (7.5%), 330 °C (11%) and 540 °C (38%) due to the loss of water molecules and decomposition of the organic part of the MOF. If the plateau in the 550 °C to 1200 °C temperature range is assumed to be 6 ZrO₂ (MW = 123 g/mol), we can use this value as reference (100 %) for extrapolating the theoretical formula from the analysis. The normalized weight at 100 °C is therefore 213%. The experimental formula weight from TGA analysis at 100 °C is therefore 1572 g/mol. Being the mass of the defective, desolvated MOF of formula Zr₆O₄(OH)₄(BDC)_{4.58}(FA)_{2.74} = 1555 g/mol, this is in good agreement with the experimental data from TGA analysis.

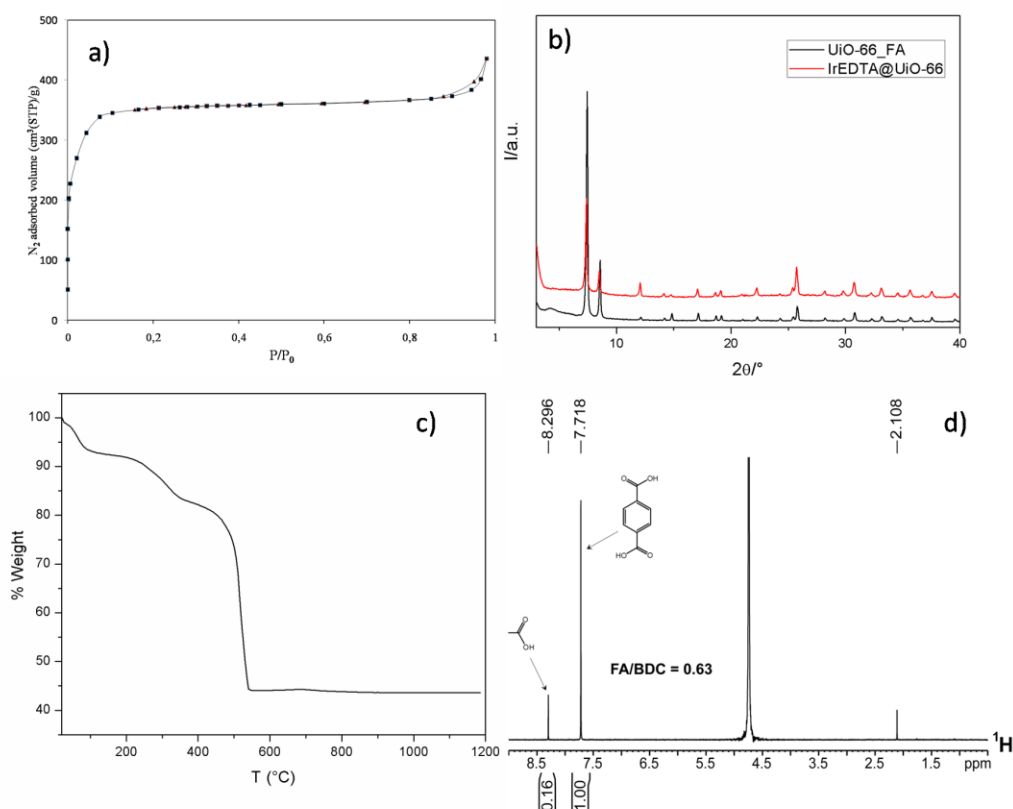


Figure 3. N_2 adsorption and desorption isotherm (a). XRPD patterns of FA_UiO-66 (black) and Ir-EDTA@UiO-66(1) (red) (b). TGA curve for FA_UiO-66 (c) and 1H -NMR spectrum for hydrolyzed FA_UiO-66 MOF (NaOD/D₂O, 298 K).

2.1.2 Synthesis of IrEDTA@UiO-66

The PSE process for anchoring the Ir-EDTA complex onto the cluster surface is shown in figure 4. After soaking the evacuated MOF into a water solution containing the dissolved complex (0.02 M) and heating at 80°C for 24 h, the partial exchange of FA with the free carboxylic group of the complex occurred.

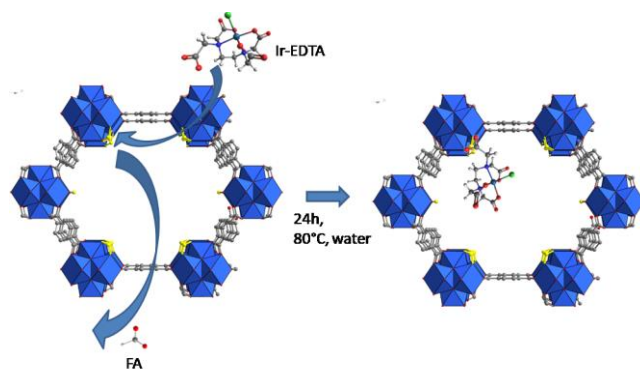


Figure 4. PSDE of FA with Ir-EDTA complex

Three samples with different amount of exchanged Ir-EDTA were prepared: The first compound Ir@UiO-66(1), (2) and (3) were exchanged with 0.096, 0.077 and 0.057 mmol of Ir-EDTA, respectively.

ICP-OES analysis for the determination of Ir content gave the following results: IrEDTA@UiO-66(1) = 256 $\mu\text{mol/g}$; IrEDTA@UiO-66(2) = 226 $\mu\text{mol/g}$ and IrETA@UiO-66(3) = 170 $\mu\text{mol/g}$. The XRPD patterns of the three samples are shown in figure 5. Anchoring Ir-EDTA onto the cluster surface did not affect the structure of the MOF since the characteristic peaks remained unaltered.

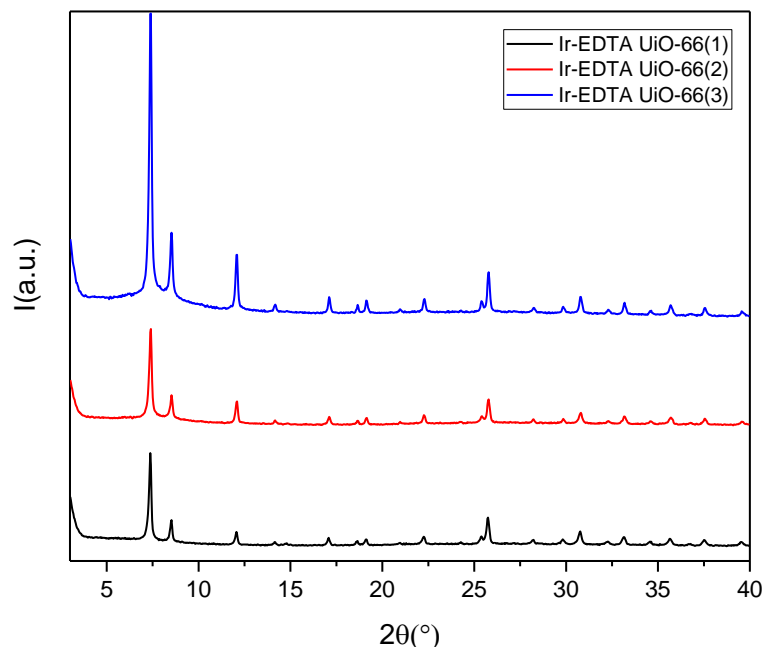


Figure 5. XRPD pattern of Ir-EDTA@UiO66(1), black, (2) red and (3) blue.

Figure 6 shows the $^1\text{H-NMR}$ spectrum of the hydrolyzed Ir@UiO-66(1) sample. The peak at 8.3 ppm attributed to FA exhibits a reduced intensity and the integration with that of BDC gave as result FA/BDC = 0.10. This value is about 6 times lower than the unmodified defective MOF (FA/BDC = 0.63) meaning that the most part of FA was successfully exchanged by Ir-EDTA complex. Peaks belonging Ir-EDTA complex are clearly visible at 3 and 2.2 ppm. With this new ratio the calculated formula becomes $\text{Zr}_6\text{O}_4(\text{OH})_4(\text{BDC})_{4.58}(\text{FA})_{0.5}(\text{Ir-EDTA})_{2.24}$

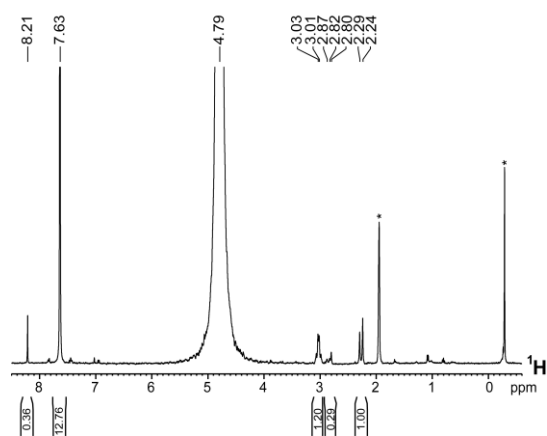
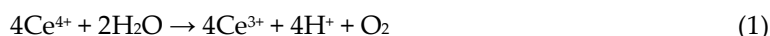


Figure 6. $^1\text{H-NMR}$ spectrum of hydrolyzed Ir@UiO-66(1) sample [NaOD/D₂O, 298 K; * denote impurities present in the solvent, likely acetone (ca 2 ppm) and TMS (slightly lower than 0 ppm)].

2.3 Water oxidation catalytic activity of IrEDTA@UiO-66

Herein, the catalytic activity of IrEDTA@UiO-66 hybrid materials toward water oxidation to molecular oxygen (Eq. 1) is described. Catalytic tests were carried out by using Ce⁴⁺ (added as CAN) as a sacrificial oxidant, dispersing the proper amount of catalyst in acidic water (pH 1, 0.1 M HNO₃) at 25 °C.



The evolved gas, according to Eq. 1, was quantified by differential manometry (Experimental Section). In a first series of experiments, a consecutive triple addition (100 µl, 150 µl and 500 µl) of a 1.25 M solution of CAN to 4.9 ml of a 51.5 µM IrEDTA@UiO-66 suspension was executed (Table 1, entries 1-3; Figure 7). IrEDTA@UiO-66 was found to be a competent catalyst for water oxidation and exhibited a TOF of ca. 5 min⁻¹ and TON values included between 62 and 308 with (yields = 30-50 %). A second series of measurements was performed with the aim of evaluating possible leaching of the molecular catalyst from the MOF support. Particularly, a catalytic run was executed by using 73.12 µM IrEDTA@UiO-66 and 75 mM CAN (Table 1, entry 4). At the end of O₂ evolution IrEDTA@UiO-66 was recovered by filtration and the supernatant solution tested by the addition of another aliquot of 75 mM CAN (Table 1, entry 5). Also the recovered solid was tested under the same conditions (Table 1, entry 6). At the end of the reaction the solid catalyst was again recovered by filtration and the second supernatant tested (Table 1, entry 7). The measured TOF (4 min⁻¹) and TON (108, yield = 42 %) values of the starting IrEDTA@UiO-66 are nicely consistent with those observed in the first series of experiments. Also the recovered solid IrEDTA@UiO-66 exhibits similar TOF (6 min⁻¹) and TOF (180, yield = 67 %) values. Nevertheless, the two supernatants are active, with even higher TOF (10 min⁻¹ and 13 min⁻¹) but comparable TON (363, yield = 44% and 1013, yield = 46 %) values, evidencing some leaching of iridium in solution. ICP-OES measurements indicate that 30.98 % and 30.75 % of iridium leached out from IrEDTA@UiO-66 after the first and second catalytic run, respectively.

The catalytic activity of IrEDTA@UiO-66 well compare with those of the molecular precursor^[34] and hybrid material IrEDTA@TiO₂^[20] tested under similar conditions, in terms of TOF (Table 1, entries 8-10 and 12). The TON values are clearly lower than those observed for the molecular precursor, which provide 100 % yield, and somewhat smaller also than those of IrEDTA@TiO₂ (Table 1, entries 8-10 and 12). Nevertheless, the main criticality of IrEDTA@UiO-66 seems to be the leaching of iridium, occurring also after the second catalytic run, contrary to what observed for IrEDTA@TiO₂ (Table 1, entries 11 and 13) and other heterogenized iridium catalysts reported before.^{[20],[17]} Several explanations might be provided for such a phenomenon. It can be hypothesized some Ce⁴⁺ might undergo an exchange with the Zr⁴⁺ ions of MOF, becoming not anymore available for driving the oxidative splitting of water. Alternatively, it might be hypothesized that the oxidative potential of iridium in IrEDTA@UiO-66 is slightly higher than in the molecular precursor and hybrid material IrEDTA@TiO₂, thus asking for a higher Ce⁴⁺/Ce³⁺ ratio in order to reach the appropriate "Nernstian" potential for WO.^[36] Both the explanations are consistent with the observation that the addition of a second aliquot of CAN restores the catalytic activity.

A catalytic run with a large amount of IrEDTA@UiO-66 (50 mg, 2.61 mM; CAN = 75 mM) was performed in order to recover and analyse IrEDTA@UiO-66 post-catalysis. The ¹H NMR spectrum of the recovered solid digested in NaOD is significantly different than that before catalysis (Figure 8). In particular, the typical resonances of the -CH₂ protons of EDTA in the 2.0 – 3.2 ppm are not anymore visible in the post-catalysis sample, suggesting a complete degradation of the ligand framework.^[37] Because the recovered solid is still active in WO, it might be hypothesized that after EDTA-degradation some iridium remains attached at the MOF structure, possibly through the formation of Zr–O–Ir oxo bridges, as observed in heterogenized WOCs prepared by anchoring an Ir-Kläui molecular precursor onto BiVO₄ nanopyramids.^[17]

Table 1. Summary of the WO catalytic data for Eq. 1.

Entry		[Ir] μM	[CAN] mM	d[O ₂]/dt mM/min	TOF min ⁻¹	TON	yield %
IrEDTA@UiO-66							
1	Run I	50	25	0.23	5	67	54
2	Run II	49	38	0.19	4	32	33
3	Run III	45	126	0.29	6	382	55
4	Run I	73	75	0.31	4	108	42
5	Sur I	23	75	0.22	10	363	44
6	Run II	70	75	0.41	6	180	67
7	Sur II	9	75	0.11	13	1013	46
IrEDTA^[34]							
8	Run I	5	80		7	4000	100
9	Run II	5	20		7	1000	100
IrEDTA@TiO₂^[20]							
10	Run I	35	9		4	46	70
11	Sur I	10	9		7	141	59
12	Run II	25	9		4	78	83
13	Sur II	0	10		–	–	–

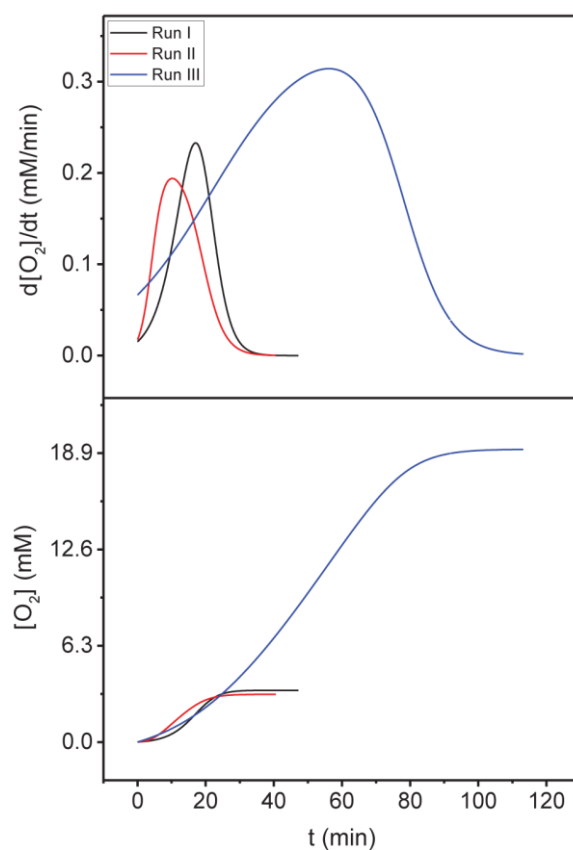


Figure 7. [O₂] (bottom) and d[O₂]/dt (up) versus time trends for a WO triple CAN addition experiment (Table 1, entries 1-3).

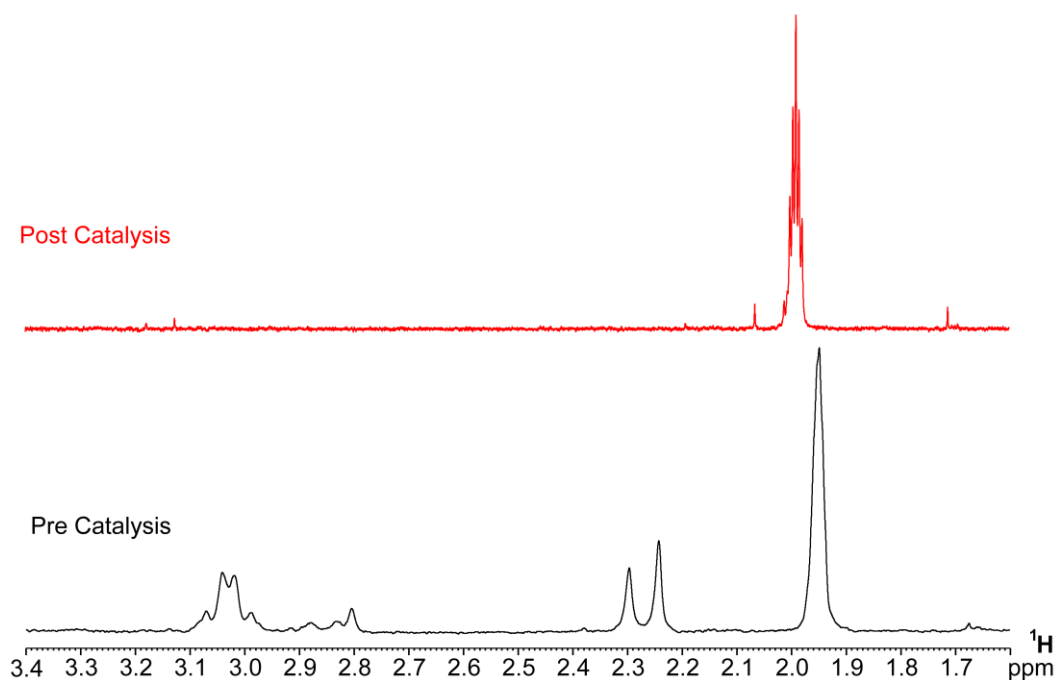


Figure 8. ^1H NMR spectra (NaOD/D₂O, 298K) before (bottom) and after (up) a catalytic run, showing the disappearance of the aliphatic resonance of the EDTA ligand at 2.0 – 3.2 ppm.

Experimental Section

4. Materials and Methods

4.1 Synthetic procedures

All reagents were used as received without further purification: ZrCl₄, Cerium Ammonium Nitrate (CAN), Formic acid (FA), Terephthalic acid (BDC) and N,N-Dimethylformamide (DMF) was purchased from Sigma Aldrich (St. Louis, MO, USA). [Ir(HEDTA)Cl]Na was prepared according to ref [34].

Synthesis of FA-UiO-66

ZrCl₄ (0.60 g, 2.5 mmol) was dissolved in DMF (40 mL). Then, water (0.135 mL, 7.5 mmol), FA (9.4 mL, 250 mmol) and bdc (0.435 g, 2.5 mmol) were added to the solution. The mixture was sonicated until complete dissolution and divided in 4 vials (10 ml each) and heated into an oven at 120 °C for 16h. After the reaction, the solid was recovered for centrifugation and washed with DMF (one time after 2h soaking), water (2h soaking) and acetone (one time after 10 min soaking). At the end, the solid was dried in an oven at 80 °C for 2h.

Synthesis of IrEDTA@UiO-66 via PSDE

FA_UiO66 (60 mg) was suspended in 5 ml of a 0.02 M water solution of a [Ir(HEDTA)Cl]Na (0.02M) for 24 hours at 80 °C. After completion of the reaction, the solid was centrifuged and washed with DMF (one time two-hour soaking), water (two times two-hour soaking) and acetone (two times two-hour soaking). The solid was dried in an oven at 80 °C for two hours. Two other syntheses with different Ir content were carried out: 30 mg of UiO-66 in 0.01M Ir-EDTA solution (5 mL) and 40 g in 0.015 Ir-EDTA solution (5 mL.)

4.2 Analytical and instrumental procedures.

Powder X-Ray Diffraction (PXRD). PXRD patterns were collected in reflection geometry in the 4-40° 2 θ range, with a 40 s step-1 counting time and with a step size of 0.016° on a PANalytical X'PERT PRO diffractometer (Malvern Panalytical Ltd., Malvern, UK), PW3050 goniometer, (Malvern Panalytical Ltd., Malvern, UK) equipped with an X'Celerator detector (Malvern Panalytical Ltd., Malvern, UK) by using the Cu K α radiation. The long fine focus (LFF) ceramic tube operated at 40 kV and 40 mA.

Thermogravimetric analysis (TGA). TGA was performed using a Netzsch STA490C thermoanalyzer (NETZSCH Group, Selb, Germany) under a 20 mL min⁻¹ air flux with a heating rate of 10 °C min⁻¹.

Nitrogen adsorption and desorption isotherms. N₂ adsorption/desorption isotherms were performed using a Micromeritics ASAP 2010 analyser (Micromeritics, Norcross, GA, USA). Prior to the analysis, the samples were degassed overnight under vacuum at 120 °C. B.E.T. analysis and t-plot analysis of the adsorption data were used to calculate specific surface area and micropore volume respectively. Harkins and Jura equation was used as reference for the statistical thickness calculation.

Ion-Chromatography Analysis. Ion chromatography was made using a Dionex 500 (Dionex Corp. Sunnyvale, USA) apparatus with a CD20 suppressed conductivity module. Sample analysis was performed as follows: About 30 mg of sample was dispersed in 40 mL of NaOH 0.0125 M and refluxed for 2 hours. After reflux, the solution was diluted to 100 mL by water. The resulting solution was analysed by ion chromatography using a Dionex AS11 column and eluted with a flux of 1.5 mL/min with NaOH 6 mM in the case of BDC analysis or NaOH 0.1 mM in the case of FA analysis.

ICP-OES Analysis. The ICP-OES analysis was carried out using a Varian 700-ES series (Agilent Technologies, Santa Clara, USA) with a standard (2, 5, 7, 10 mg/L respectively) of Iridium solution.

WO catalytic experiments. Catalytic experiments were performed using two homemade jacketed glass reactors coupled to a Testo 521-1 manometer. In a typical catalytic run, IrEDTA@UiO-66 suspended in a 0.1 M HNO₃ solution was loaded into the first reaction vessel (working cell), whereas an equal amount of neat water was loaded into the second one (reference cell). Both reactors were sealed with a rubber septum, connected to the manometer, kept at a constant temperature of 25 °C and placed under stirring for 20 minutes. Acquisition was started. When a steady baseline was achieved, an equal volume of a solution of CAN and neat water were injected into the working cell and reference cell, respectively, to reach a final volume of 5 mL in each reactor. The concentration of the stock solution of CAN was adjusted, depending on the final concentration desired, in order to have a maximum injection volume of 500 μ L. The total gas evolved was estimated by measuring the differential pressure between the working and reference cell.

Fitting methodology and kinetic data analyses. All trends of [O₂] evolution *versus* time were fitted by a composite mathematical function developed by Peters and Baskin (PB) for distinguishing sigmoidal and bilinear growth profiles of plant roots.^[88] The derivative of the PB fits provided reaction rate ($v = d[O_2]/dt$) trends as function of time. Reaction rate over catalyst concentration led to TOF ($= v/[Ir]$), which was plotted versus the factor conversion $X (= 4[O_2]/[CAN]_0)$.^[91]

5. Conclusions

In this paper a catalytic active Ir complex based on EDTA was successfully anchored onto a defective Zr-MOF with UiO-66 structure. The post-synthetic modification of defective MOF for designing a new heterogeneous catalyst was here validated for the first time demonstrating that substitution of small formate anions linked to zirconium clusters with larger carboxylate-bearing complex is possible. The material was employed for water oxidation reaction using Ce⁴⁺ as sacrificial agent. The catalyst showed a good catalytic activity, comparable to that observed for other heterogenized catalysts. However, Ir-leaching occurs not only during the first catalytic run, as usually observed, but also for the successive ones. This fact suggests that the material is not stable under the strong oxidative conditions due to the high redox potential of Ce⁴⁺. Furthermore, the WO reaction yield is somewhat lower than that observed for other heterogenized iridium WOCs, indicating a possible exchange of the zirconium atom of MOF with cerium of CAN or a higher "Nernstian"

potential. Despite those drawbacks, the results reported in this paper suggest that anchoring a molecular WOC onto a defective MOF is a viable strategy to assemble hybrid material to be integrated into a device for the generation of renewable fuels.

References

- [1] J. H. Alstrum-Acevedo, M. K. Brennaman, T. J. Meyer, *Inorg. Chem.* **2005**, *44*, 6802–6827.
- [2] N. S. Lewis, D. G. Nocera, *Proc. Natl. Acad. Sci.* **2006**, *103*, 15729 LP – 15735.
- [3] V. Balzani, A. Credi, M. Venturi, *ChemSusChem* **2008**, *1*, 26–58.
- [4] A. Llobet, *Molecular Water Oxidation Catalysis: A Key Topic for New Sustainable Energy Conversion Schemes*, Wiley-Interscience: New York, **2014**.
- [5] A. Macchioni, *Eur. J. Inorg. Chem.* **2019**, *2019*, 7–17.
- [6] I. Corbucci, A. Macchioni, M. Albrecht, in *Iridium Optoelectron. Photonics Appl.*, John Wiley & Sons Ltd., **2017**, pp. 617–654.
- [7] J. M. Thomsen, D. L. Huang, R. H. Crabtree, G. W. Brudvig, *Dalt. Trans.* **2015**, *44*, 12452–12472.
- [8] G. Menendez Rodriguez, A. Bucci, R. Hutchinson, G. Bellachioma, C. Zuccaccia, S. Giovagnoli, H. Idriss, A. Macchioni, *ACS Energy Lett.* **2017**, *2*, 105–110.
- [9] A. Macchioni, G. Menendez Rodriguez, G. Gatto, C. Zuccaccia, *ChemSusChem* **2017**, 4503–4509.
- [10] T. K. Michaelos, D. Y. Shopov, S. B. Sinha, L. S. Sharninghausen, K. J. Fisher, H. M. C. Lant, R. H. Crabtree, G. W. Brudvig, *Acc. Chem. Res.* **2017**, *50*, 952–959.
- [11] K. R. Yang, A. J. Matula, G. Kwon, J. Hong, S. W. Sheehan, J. M. Thomsen, G. W. Brudvig, R. H. Crabtree, D. M. Tiede, L. X. Chen, et al., *J. Am. Chem. Soc.* **2016**, *138*, 5511–5514.
- [12] J. A. Woods, R. Lalrempuia, A. Petronilho, N. D. McDaniel, H. Muller-Bunz, M. Albrecht, S. Bernhard, *Energy Environ. Sci.* **2014**, *7*, 2316–2328.
- [13] A. Venturini, A. Barbieri, J. N. H. Reek, D. G. H. Hetterscheid, *Chem. - A Eur. J.* **2014**, *20*, 5358–5368.
- [14] N. D. McDaniel, F. J. Coughlin, L. L. Tinker, S. Bernhard, *J. Am. Chem. Soc.* **2008**, *130*, 210–217.
- [15] M. Li, K. Takada, J. I. Goldsmith, S. Bernhard, *Inorg. Chem.* **2016**, *55*, 518–526.
- [16] L. Fagiolari, A. Scafuri, F. Costantino, R. Vivani, M. Nocchetti, A. Macchioni, *Chempluschem* **2016**, *81*, 1060–1063.
- [17] X. Wan, L. Wang, C.-L. Dong, G. Menendez Rodriguez, Y.-C. Huang, A. Macchioni, S. Shen, *ACS Energy Lett.* **2018**, *3*, 1613–1619.
- [18] S. W. Sheehan, J. M. Thomsen, U. Hintermair, R. H. Crabtree, G. W. Brudvig, C. A. Schmuttenmaer, *Nat. Commun.* **2015**, *6*, DOI 10.1038/ncomms7469.
- [19] Z. Chen, J. J. Concepcion, X. Hu, W. Yang, P. G. Hoertz, T. J. Meyer, *Proc. Natl. Acad. Sci. U. S. A.* **2010**, *107*, 7225–7229.
- [20] A. Savini, A. Bucci, M. Nocchetti, R. Vivani, H. Idriss, A. Macchioni, *ACS Catal.* **2015**, *5*, 264–271.
- [21] G. Pastori, K. Wahab, A. Bucci, G. Bellachioma, C. Zuccaccia, J. Llorca, H. Idriss, A. Macchioni, *Chem. - A Eur. J.* **2016**, *22*, 13459–13463.
- [22] K. L. Materna, B. Rudshiteyn, B. J. Brennan, M. H. Kane, A. J. Bloomfield, D. L. Huang, D. Y. Shopov, V. S. Batista, R. H. Crabtree, G. W. Brudvig, *ACS Catal.* **2016**, *6*, 5371–5377.
- [23] K. L. Materna, R. H. Crabtree, G. W. Brudvig, *Chem. Soc. Rev.* **2017**, *46*, 6099–6110.
- [24] C. Wang, Z. Xie, K. E. DeKrafft, W. Lin, *J. Am. Chem. Soc.* **2011**, *133*, 13445–13454.
- [25] C. Wang, J. L. Wang, W. Lin, *J. Am. Chem. Soc.* **2012**, *134*, 19895–19908.
- [26] Q. Shao, J. Yang, X. Huang, *Chem. - A Eur. J.* **2018**, *24*, 15143–15155.

- [27] K. Adil, Y. Belmabkhout, R. S. Pillai, A. Cadiau, P. M. Bhatt, A. H. Assen, G. Maurin, M. Eddaoudi, *Chem. Soc. Rev.* **2017**, *46*, 3402–3430.
- [28] Z. Chen, K. Adil, Ł. J. Weseliński, Y. Belmabkhout, M. Eddaoudi, *J. Mater. Chem. A* **2015**, *3*, 6276–6281.
- [29] J. Escorihuela, R. Narducci, V. Compañ, F. Costantino, *Adv. Mater. Interfaces* **2019**, *6*, 1801146.
- [30] P. Silva, S. M. F. Vilela, J. P. C. Tomé, F. A. Almeida Paz, *Chem. Soc. Rev.* **2015**, *44*, 6774–6803.
- [31] J. H. Cavka, S. Jakobsen, U. Olsbye, N. Guillou, C. Lamberti, S. Bordiga, K. P. Lillerud, *J. Am. Chem. Soc.* **2008**, *130*, 13850–13851.
- [32] M. Taddei, *Coord. Chem. Rev.* **2017**, *343*, 1–24.
- [33] M. Taddei, R. J. Wakeham, A. Koutsianos, E. Andreoli, A. R. Barron, *Angew. Chemie Int. Ed.* **2018**, *57*, 11706–11710.
- [34] A. Savini, G. Bellachioma, S. Bolaño, L. Rocchigiani, C. Zuccaccia, D. Zuccaccia, A. Macchioni, *ChemSusChem* **2012**, *5*, 1415–1419.
- [35] M. R. DeStefano, T. Islamoglu, S. J. Garibay, J. T. Hupp, O. K. Farha, *Chem. Mater.* **2017**, *29*, 1357–1361.
- [36] Z. Codolà, I. Gamba, F. Acuña-Parés, C. Casadevall, M. Clémancey, J.-M. Latour, J. M. Luis, J. Lloret-Fillol, M. Costas, *J. Am. Chem. Soc.* **2019**, *141*, 323–333.
- [37] C. Zuccaccia, G. Bellachioma, O. Bortolini, A. Bucci, A. Savini, A. Macchioni, *Chem. - A Eur. J.* **2014**, *20*, 3446–3456.
- [38] W. S. Peters, T. I. Baskin, *Plant Methods* **2006**, *2*, 11.

Author Contributions: conceptualization, F.C and A.M.; methodology, F.C. F.M. A.M.; formal analysis, G.G., R.B. and F.M.; data curation, G.G. F.M. and F.C.; writing—original draft preparation, F.C. and A.M.; writing—review and editing, F.C. and A.M.

Funding: This research was funded by PRIN 2015 (20154X9ATP_004) and University of Perugia and MIUR (AMIS, “Dipartimenti di Eccellenza - 2018-2022” program). G. G. thanks Regione Umbria - “Umbria A.R.C.O.” for a post-doc grant. Authors also thanks Forndo Ricerca di Base 2017 (FRB2017) University of Perugia for the financial support.

Conflicts of Interest: The authors declare no conflict of interest.

